Oscillatory Activity in Human Parietal and Occipital Cortex Shows Hemispheric Lateralization and Memory Effects in a Delayed Double-Step Saccade Task

W. Pieter Medendorp[1,2], Geerten F.I. Kramer[1,2], Ole Jensen[2], Robert Oostenveld[2], Jan-Mathijs Schoffelen[2,3] and Pascal Fries[2,3]

[1]Nijmegen Institute for Cognition and Information, [2]F.C. Donders Centre for Cognitive Neuroimaging and [3]Department of Biophysics, Radboud University Nijmegen, NL-6500 HE Nijmegen, The Netherlands

We applied magnetoencephalography (MEG) to record oscillatory brain activity from human subjects engaged in planning a double-step saccade. In the experiments, subjects (*n* = 8) remembered the locations of 2 sequentially flashed targets (each followed by a 2-s delay), presented in either the left or right visual hemifield, and then made saccades to the 2 locations in sequence. We examined changes in spectral power in relation to target location (left or right) and memory load (one or two targets), excluding error trials based on concurrent eye tracking. During the delay period following the first target, power in the alpha (8–12 Hz) and beta (13–25 Hz) bands was significantly suppressed in the hemisphere contralateral to the target. When the second target was presented, there was a further suppression in the alpha- and beta-band power over both hemispheres. In this period, the same sensors also showed contralateral power enhancements in the gamma band (60–90 Hz), most significantly prior to the initiation of the saccades. Adaptive spatial filtering techniques localized the neural sources of the directionally selective power changes in parieto-occipital areas. These results provide further support for a topographic organization for delayed saccades in human parietal and occipital cortex.

Keywords: human, MEG, oscillations, parietal cortex, saccade, sensorimotor, spatial memory

Introduction

The delayed-saccade task is an important tool for studying working memory processes in the brain. In this task, a subject fixates a central target while a light is flashed onto the retinal periphery; then, after a short time interval, he or she is cued to look at the remembered location of the flash. Several cortical and subcortical regions, in both human and nonhuman primates, have been shown to retain increased activity during the memory interval until the saccade is made (see Pierrot-Deseilligny et al. 2004 for review).

In the monkey, one of these regions is the lateral intraparietal area (LIP) (Barash et al. 1991; Colby et al. 1996; Mazzoni et al. 1996) located in the posterior parietal cortex, and recognized as an important interface between higher-order visual areas and the oculomotor system (Andersen and Buneo 2002). Increased firing rate in this region has not only been associated with the planning of saccades but also with sensory attention, decision making, and spatial updating. Some studies have reported that neurons in LIP are arranged in a topographical order, preferentially representing target locations from the contralateral visual field (Blatt et al. 1990; Ben Hamed et al. 2001, but see Platt and Glimcher 1998).

Recently, functional magnetic resonance imaging (fMRI) studies have identified a putative human equivalent of monkey area LIP by describing a bilateral region within the posterior superior parietal lobule that topographically represents remembered target locations for delayed saccades (Sereno et al. 2001; Medendorp et al. 2003, 2005; Koyama et al. 2004; Schluppeck et al. 2005). It was further shown that the directionally selective activity in human LIP is modulated with memory load in a double-saccade task, which implicates the region in the active maintenance of multiple target locations (Medendorp et al. 2006). Notably, most of these fMRI studies also reported other regions showing directional selectivity for delayed saccades (Schluppeck et al. 2005). One region of particular interest was identified in anterior-occipital cortex (Sereno et al. 2001; Medendorp et al. 2003, 2005) possibly corresponding to monkey extrastriate area V3A, which has been shown to carry memory and saccade-related signals as well (Nakamura and Colby 2000).

Yet, sustained blood oxygen level–dependent (BOLD) signals or increased firing rates are not the only signatures of ongoing neural activity in these regions. Neural processing is also characterized by both event-related and oscillatory signals, which can be recorded as electroencephalography (EEG) or MEG from the scalp. Given that the oscillatory signals are produced by large ensembles of neurons oscillating in synchrony, they are bound to play an important role in neuronal processing (see Hari and Salmelin 1997; Engel et al. 2001, for reviews). In both human and nonhuman primates various reports have linked the internal rhythms generated within distinct regions of the brain to memory maintenance in various types of working memory tasks. Oscillations in the theta (4–8 Hz) and gamma band (30–80 Hz) have been associated with neuronal activity responsible for active memory maintenance, whereas alpha-band (8–12 Hz) activity has been proposed to reflect inhibition of regions not required for the memory task (Tallon-Baudry et al. 1996, 2001; Gevins et al. 1997; Klimesch et al. 1999; Jensen et al. 2002; Lutzenberger et al. 2002; Pesaran et al. 2002; Howard et al. 2003; Kaiser et al. 2003; Lee et al. 2005; Scherberger et al. 2005).

The present study was carried out to characterize human oscillatory brain activity during the memory period in a delayed double-saccade task. More specifically, we addressed the question whether the neural mechanisms that give rise to the spatially selective and load-dependent BOLD activity observed in human extrastriate and parietal regions (Medendorp et al. 2006) would be reflected by similar modulations of oscillatory activity, originating from neural sources at corresponding locations.

To our knowledge, spatially tuned spectral activity in relation to memory-guided saccades has not been demonstrated in human subjects. In close connection though, using a spatial attention task, Worden et al. (2000) demonstrated a lateralized power distribution in the alpha band (8–12 Hz), in EEG sensors overlying occipital cortex. Although it is unclear whether the

same neural sources are involved in coding targets for delayed saccades, these data show that spatial-tuning effects on oscillatory activities can be measured noninvasively. Okada and Salenius (1998), who performed a single saccade task in MEG, observed strong alpha effects over occipital and parietal sensors but they did not address the issue of laterality or target load. Neither Okada and Salenius (1998) nor Worden et al. (2000) have identified the source locations of the alpha-band activity.

Here, we investigated oscillatory brain activity with magnetoencephalography (MEG), applying a slightly modified version of the delayed double-saccade paradigm used by Medendorp et al. (2006). This task has proven effective in dissociating target load and spatial selectivity for delayed saccades in fMRI. We examined spectral power while subjects saw 2 brief visual targets, separated by a short time interval, in either the left or right visual hemifield. Subjects were required to memorize these 2 target locations and, after another delay, made saccades to them in sequence. Our results show that the strength of spectral power at various posterior sensors was modulated by the number of target locations kept in memory as well as by the location of these targets within the visual hemifield. Using adaptive spatial filtering techniques, we localized the sources of the oscillatory activity in posterior parietal and occipital cortex.

Materials and Methods

Subjects

Eight healthy paid volunteers (5 males, 3 females, mean age of 23 years) participated in the experiments. All subjects gave their written informed consent in accordance with the institutional guidelines of the local ethics committee (CMO Committee on Research Involving Human Subjects, region Arnhem-Nijmegen, The Netherlands). Each subject practiced all tasks extensively before data acquisition to ensure that the tasks were performed correctly. Moreover, eye movement recordings and psychophysical measures were taken to confirm accurate behavior, as described below.

Experimental Setup

Subjects were seated upright in the MEG system that was placed in a magnetically shielded room. They were instructed to sit comfortably but still, and to look at the stimulus screen, positioned at about 40 cm in front of them. Visual stimuli, generated with Presentation 9.10 software (Neurobehavioral Systems Inc., Albany), were presented using an LCD video projector (SANYO PROxtraX mutiverse, 60-Hz refresh rate) and back-projected onto the screen using 2 front-silvered mirrors. MEG data were recorded continuously using a whole-head system with 151 axial gradiometers (Omega 2000, CTF Systems Inc., Port Coquitlam, Canada). Head position with respect to the sensor array was measured using localization coils fixed at anatomical landmarks (the nasion and at the left and right ear canal). These measurements were made before and after the MEG recordings to assess head movements during the experiment. In addition, horizontal and vertical electro-oculograms were recorded using electrodes placed below and above the left eye and at the bilateral outer canthi. Electrode impedance was kept below 20 kOhm. During the experiment, these recordings were continuously inspected to check subjects' task behavior and vigilance. MEG, electro-oculargraphy, and electrocardiography signals were low-pass filtered at 300 Hz, sampled at 1200 Hz, and then saved to disk. Subjects' psychophysical performance was recorded by means of key presses using a button box (LUMI-Touch).

For each subject, a full-brain anatomical MR image was acquired using a high-resolution inversion prepared 3D T_1-weighted scan sequence (flip angle = 15°; voxel size: 1.0 mm in-plane, 256 × 256, 164 slices, time repetition = 0.76 s; time echo = 5.3 ms). The anatomical MRIs were recorded using a 1.5-T whole-body scanner (Siemens, Erlangen, Germany), with anatomical reference markers at the same locations as the head position coils during the MEG recordings (see above). The reference markers allow alignment of the MEG and MRI coordinate systems, such that the MEG data can be related to the anatomical structures within the brain.

Experimental Paradigm

We investigated the temporal structure in human brain activity during delayed double-step saccades. Figure 1 illustrates the paradigm, which is a modified version of the fMRI paradigm used by Medendorp et al. (2006). Subjects were first asked to make an eye blink and then fixate centrally on a white cross. Subsequently, a red square (stim 1, size 0.7 × 0.7°) was flashed for 200 ms, either left or right of central fixation, at a random eccentricity between 9° and 18° and at a random angular elevation within a range of 6° and 13°, in either the lower or upper visual field. This was followed by a 2-s memory delay during which the subject maintained fixation. Then, another peripheral red square (stim 2) was flashed for 200 ms, in the same hemifield as the first stimulus. The location of the second stimulus was separated from the location of the first by at least 6° of visual angle. Subjects had to memorize the locations of both stimuli both of which were thus either right or left from the fixation direction. Next, 2 s after offset of the second stimulus, the fixation cross was turned off, prompting the subject to make saccades to the remembered locations of the stimuli, in the same sequence as they had appeared. To motivate the subjects to memorize the spatial positions accurately, memory performance was probed in the following way: Small letters, either "c" or "o," were shown from 300 to 400 ms after fixation cross offset at the original location of the first stimulus and from 600 to 700 ms after fixation cross offset at the original location of the second stimulus (not shown in Fig. 1). Due to their very small size and short appearance, the letters were distinguishable ("c" or "o") only if the subject fixated at the correct location at the right time. This in turn could only be achieved if the subjects remembered accurately the
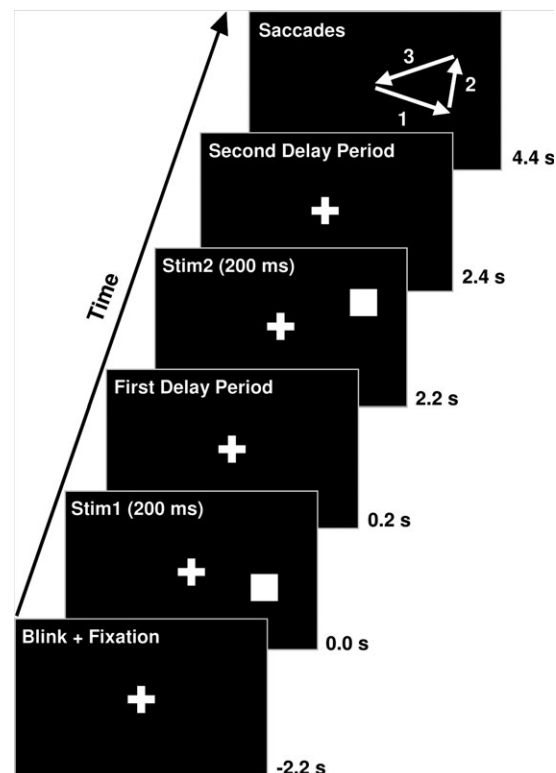

Figure 1. Experimental paradigm. Although subjects fixated centrally on a white cross, a red square (stim 1, size 0.7 × 0.7°) was flashed for 200 ms, either in the left or right hemifield. After a delay period, which lasted for 2 s, a second peripheral stimulus was flashed (stim 2, 200 ms) in the same hemifield but at least 6° apart from the location of the first cue. Then, after a further 2 s, the fixation cross disappeared instructing the subjects to look successively toward the remembered locations of the 2 stimuli, and immediately back to center. The letter stimuli and instructions related to the psychophysical measures taken (see text) are not shown.

spatial positions of the 2 original targets. The letters were sufficiently small and short lived that subjects could not base their saccades on the presentation of the letters themselves. Subsequently, the central fixation cross (Fix) was turned on again, instructing the subject to make a saccade back to the centre of the screen and fixate till the end of the trial. During this period, subjects had to report which letters they had seen by pressing the corresponding buttons on a key pad using their right hand. The subject's actual performance was determined from the eye movement recordings, described below.

In addition, subjects performed trials in which they first blinked and then fixated centrally at all times, without presentation of any stimulus. These trials had the same duration as the test trials, described above, and served as baseline of the MEG recordings in further analyses. This baseline was not intended to match the memory trials in aspects like, for example, difficulty. Rather, it was meant solely to serve as low-level baseline for the normalization of power estimates obtained in the memory trials.

The total duration of each trial was 9.35 s. Each subject performed 240 trials, consisting of 96 trials in which the 2 stimuli were flashed in the right visual field, 96 trials with stimuli in the left field and 48 baseline trials. The recording session was divided in 8 blocks of 30 trials, in which test and baseline trials were pseudorandomly interleaved. After each block of trials, subjects were given 1 min of rest, and their psychophysical performance hitherto was indicated on the screen. The total experiment lasted for 45 min.

Behavioral Analysis
As measured by the button presses, the subjects' performance on the letter detection task was over 80% correct. We did not exclude any trials based on this measure: the psychophysics was merely incorporated to motivate subjects to perform optimally. Eye movement recordings in all subjects also confirmed that they generally followed the instructions correctly: on average in 6% of the trials did the subjects either break fixation (i.e., eye movements which exceeded the noise of our recording system) or make their saccades in the wrong direction. We excluded these error trials from further analysis.

Data Analysis
Data were analyzed using Fieldtrip software (http://www.ru.nl/fcdonders/fieldtrip), an open source Matlab toolbox for EEG and MEG data analysis developed at the F.C. Donders Centre for Cognitive Neuroimaging. As indicated above, we discarded trials in which subjects failed to keep eye fixation or made eye movements in the wrong directions. From the remaining trials, data segments that were contaminated with eye blinks, muscle activity or jump artifacts in the SQUIDs were excluded using semiautomatic artifact rejection routines. Power line noise was removed using a Fourier transformation of 10-s long signal periods and subtracting the 50 Hz component and its harmonics. This was done separately for all 10-s periods around all periods of interest from the continuous data record.

We analyzed the data in the frequency domain. For the sensor-level analysis, an estimate of the planar gradient was calculated for each sensor using the signals from the neighboring sensors. The horizontal and vertical components of the planar gradients approximate the signal measured by MEG systems with planar gradiometers. The planar field gradient simplifies the interpretation of the sensor-level data if sources are superficial and dipolar because then the maximal signal is located above the source (Hamalainen et al. 1993). A further advantage of planar gradiometers is that a superficial dipole activates a contiguous set of sensors (whereas for axial gradiometers, 2 separate sets are activated). This is important for cluster-based randomization statistics, as described below. Power spectra were computed separately for the horizontal and vertical planar gradients of the MEG field at each sensor and the resultant vector length of both was computed to obtain the power at each sensor location irrespective of the orientation of the gradient. For each subject, we visually inspected the averaged power spectral densities. Following the approach suggested by Klimesch (1999), we determined individual peak frequencies for the alpha (8–12 Hz) and beta bands (13–25 Hz), as shown by Table 1.

In the actual analysis of the data, we examined the changes in spectral power in the test trials relative to the baseline trials to determine the neural response related to the task. To investigate target load effects, we

compared power differences between data epochs in which one target was memorized (first delay period 1, see Fig. 1) and data epochs in which 2 targets were kept in memory (second delay period 2). Likewise, we examined laterality effects by comparing the power in those trials in which the stimuli appeared in the left visual field with those in which stimuli were presented in the right visual field, for both the first and second memory period. We considered the power changes at various frequency bands, using the data at the individual peak frequencies when examining scalp topography across subjects (see Figs 2, 4, and 5). Using a jackknife procedure (Efron and Tibshirani 1991), we determined the variance of the power in the selected frequency bands separately for each time point across trials. Using these estimates, we expressed the difference in power between 2 conditions as a t-score separately for each subject. The resulting t-scores were transformed into z-scores and pooled across subjects to obtain a fixed-effects measure of the significance of the mean power change across subjects for each of the frequency bands. The critical value was Bonferroni corrected with the

Table 1
Peak frequencies in the alpha and beta bands in 8 subjects

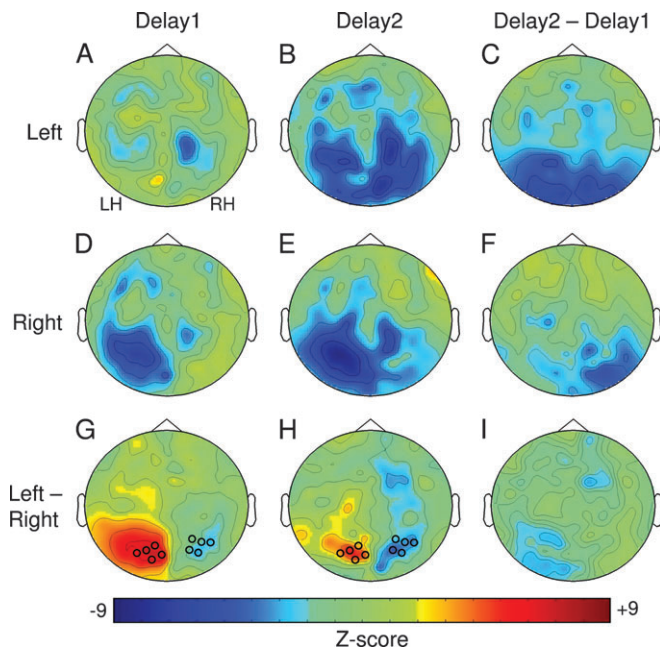| Subject	Alpha band (Hz)	Beta band (Hz)
S1	10	21.5
S2	9.5	18.5
S3	9	23.5
S4	10.5	20
S5	11.5	19
S6	9.5	17
S7	10.5	20
S8	10.5	23.5
Mean	10.1 ± 0.8 (standard deviation)	20.4 ± 2.3

Figure 2. Topographic distribution of power in the alpha band (8–12 Hz) averaged across subjects. (*A*, *B*) Suppression of the alpha-band power relative to baseline for stimuli presented in the left visual hemifield, for the first (delay 1) and second (delay 2) retention period, respectively. (*C*) Difference between delay 2 and delay 1 showing that alpha is further suppressed with target load. Middle panels, alpha-band suppression for stimuli in the right visual hemifield (*D*, *E*) and their difference (*F*). Bottom panels: contralateral suppression of alpha-band power, for both first (*G*) and second (*H*) retention period. (*I*) The degree of laterality does not increase with target load. Blue regions indicate a stronger suppression for remembered target locations in the left hemifield compared with the right. Red regions represent the opposite pattern. Open circles: positions of sensors selected in further analysis. Each map has been scaled equally between −9 < z < 9 (following the color range indicated) (|z| > 3.77, P < 0.05 Bonferroni corrected). LH/RH: left/right hemisphere.
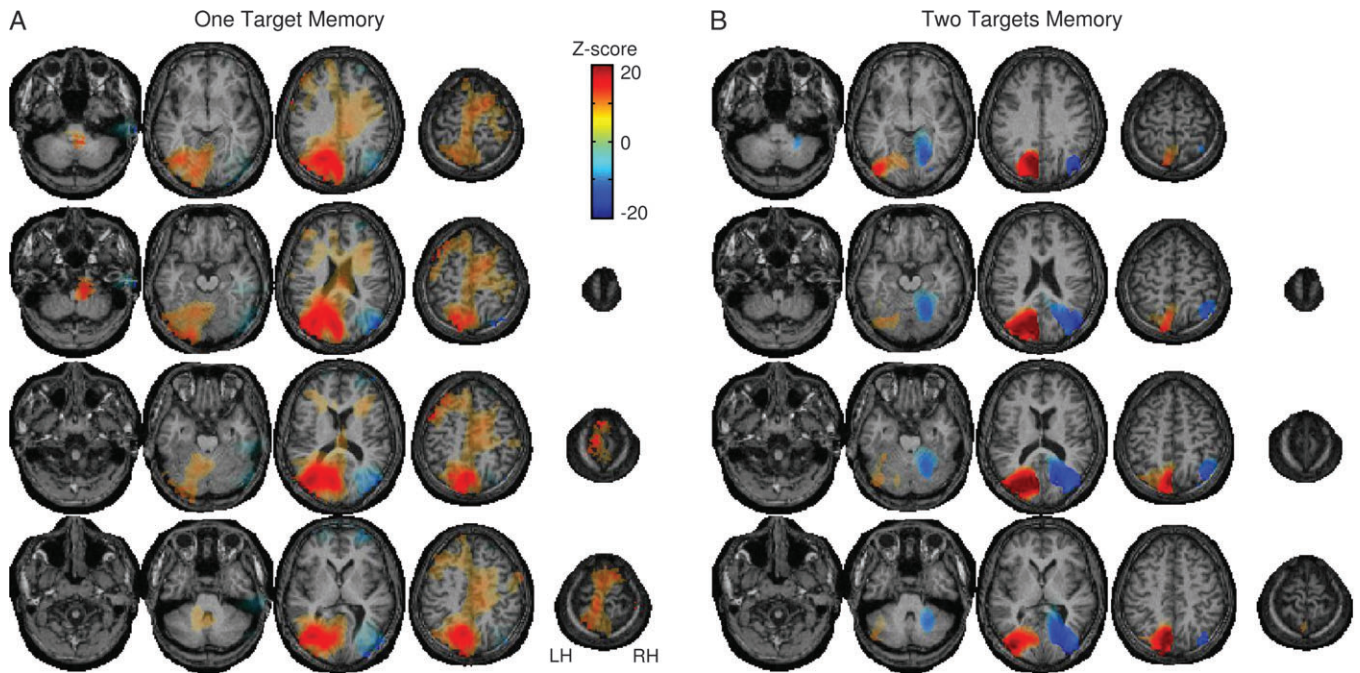
Figure 3. Regions within the posterior parietal and occipital cortex (transversal view) that show contralateral suppression effects in the alpha band during the first (*A*) and second (*B*) delay period. Population average of power difference between Target-Left and Target-Right conditions. Only significant clusters of voxels are shown (*P* < 0.05, randomization statistics with correction for multiple comparisons). The opacity of each voxel is scaled by its *z*-value. Blue regions indicate a stronger suppression for remembered target locations in the left hemifield compared with the right. Red regions represent the opposite pattern. LH/RH: left/right hemisphere.
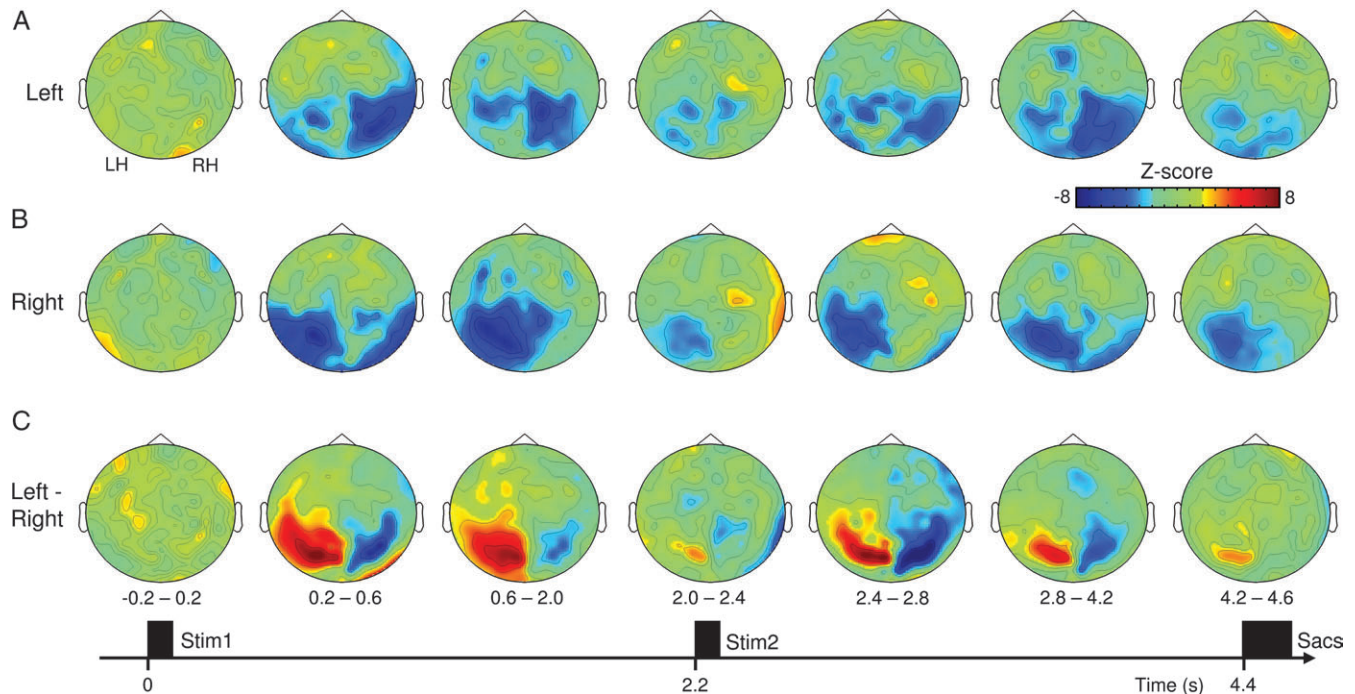

Figure 4. Temporal development of the topography in the alpha band (8–12 Hz). (*A*, *B*) Alpha-band suppression relative to baseline for stimuli in the left and right visual hemifield, respectively. (*C*) Difference in alpha-band activity between leftward and rightward stimuli showing phasic and tonic components. Blue regions indicate a stronger suppression for remembered target locations in the left hemifield compared with the right, and vice versa for red regions. ($|z|$ > 4.07, *P* < 0.05 Bonferroni corrected). LH/RH: left/right hemisphere.

number of sensors and time points, corresponding to $|z|$ > 3.77, *P* < 0.05 for Figures 2 and 5, and $|z|$ > 4.07, *P* < 0.05 for Fig. 4). We used repeated-measures analyses of variance for post hoc comparative power analysis of selected sensor groups across subjects, setting the type I error at the 0.05 level (*P* < 0.05).

Time-frequency representations (TFR), estimating the time course in power, were computed using a multitaper method. This approach seeks to optimize spectral concentration over the frequency of interest (Mitra and Pesaran 1999). We analyzed 2 frequency ranges separately: 1–30 Hz (alpha/beta) and 30–120 Hz (gamma). The lower band was analyzed
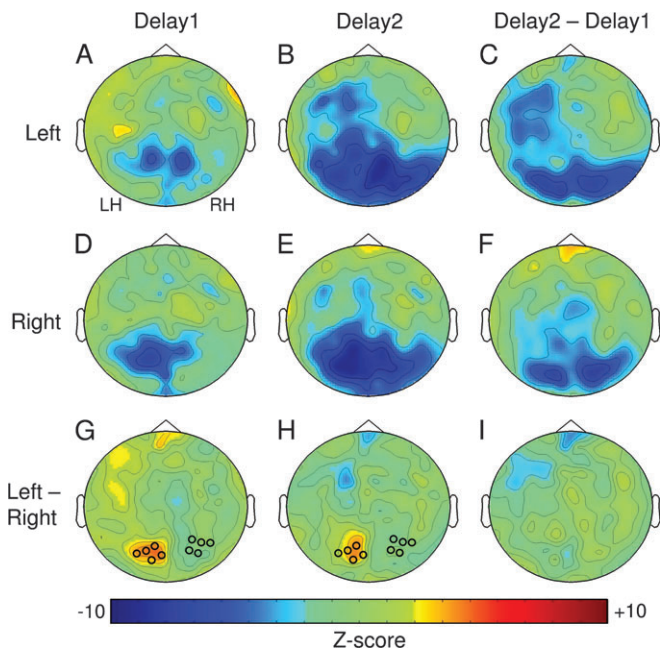
Figure 5. Contralateral suppression of power in the beta band (13–25 Hz). Data in same format as in Figure 2 ($|z| > 3.77$, $P < 0.05$ Bonferroni corrected).

using a window length of 1000 ms and a spectral smoothing of 1 Hz. The higher frequency band was analyzed using a window length of 400 ms and a spectral smoothing of 15 Hz. For each subject, power differences were expressed as a *z*-score, as described above.

Here, statistical significance was tested on the group level using a nonparametric randomization test (Nichols and Holmes 2002; Osipova et al. 2006). This test effectively controls the type I error (i.e., the false alarm rate) in a situation of multiple comparisons by clustering neighboring time–frequency points that exhibit the same effect. This is the procedure: 1) across subjects, we performed a *t*-test for all time–frequency points, using the single subject *z*-scores. 2) We selected time–frequency *t*-values that exceeded a predefined critical value. 3) We detected clusters of time–frequency *t*-values that were contiguous in time and/or frequency. 4) For each cluster, we determined the so-called cluster-level statistic, which was the sum of all *t*-values inside the cluster. 5) Applying steps (1) to (4) to the observed data provided a set of clusters with the corresponding cluster-level statistic. 6) A null distribution for the cluster-level statistic was created by performing the following steps many times: For each subject, the data were randomly reassigned over the 2 conditions, that is, all trials in one condition were randomly assigned to either one or the other condition, all trials in the other condition were assigned to the remaining condition. Then steps (1) to (4) were applied leading to a number of clusters with corresponding cluster-level statistics, from which the maximum cluster-level statistic is entered into the null distribution. 7) The cluster-level statistics found in the observed data were compared with this randomization distribution of maximum cluster-level statistics. For each cluster from the observed data, the *P* value is given as the proportion of this randomization distribution exceeding the respective cluster's test statistic.

The cluster-randomization test controls the type 1 error rate and solves the multiple comparison problem by using a single test statistic for the complete TFR (instead of one test statistic for each time–frequency point separately within the TFR). In addition, the procedure implements a test for so-called random effects because the randomization is done at the level of subjects and not at the level of individual trials.

To localize the neural sources of the alpha-band activity (as shown by Fig. 3), we applied an adaptive spatial filtering or "beamforming" technique (Gross et al. 2001; Hoogenboom et al. 2006). Each subject's brain volume was divided into a regular 8-mm 3D grid. For each grid point, a spatial filter was constructed that passes activity originating from this location with unity gain, whereas attenuating activity originating at other locations (Van Veen et al. 1997). This filter was computed using a forward model of a dipole source at the location of interest (the leadfield matrix) and the cross-spectral density between all combinations of sensors at the frequency of interest (see Bauer et al. 2006 for a detailed description of this procedure). We used a multispherical volume conductor model to compute the leadfield matrix by fitting a sphere to the head surface underlying each sensor (Huang and Mosher 1997). The head shape was derived from each individual structural MRI. We used the stimulus-induced power changes at the selected peak frequencies, as specified separately for each frequency band and each individual subject, to optimally capture the effect of interest. We used a *z*-statistic to express the power effects at the source level.

Using SPM2 (http://www.fil.ion.ucl.ac.uk/spm), the individual anatomical MRIs and the corresponding statistical maps were spatially normalized to the International Consortium for Brain Mapping template (Montreal Neurological Institute, Montreal, Canada). The individual spatially normalized statistical maps were subsequently pooled to obtain a fixed effect statistic using the same procedure as for the sensor data. Multiple comparison corrections at the source level were made by applying a 3D cluster-randomization analysis (which operates along the lines described above for the TFR cluster-randomization analysis).

Results

We investigated the modulations of oscillatory activity with target location and target load in a double-delayed double-saccade task. In this task, subjects first saw the target of the first saccade, then, after a 2-s delay, the target for the second saccade and then, after another 2-s delay, they made saccades successively to the remembered stimulus locations (see Fig. 1). The paradigm had 2 different conditions of interest regarding the locations of the 2 targets: both were cued either in the right visual field (Target-Right condition) or in the left visual field (Target-Left condition).

As a first step in our analysis, we determined the scalp topography of the changes in power in the alpha band (8–12 Hz) (expressed as a *z*-score) for the 2 memory periods (always excluding the first 400 ms after target offset in order to reduce contributions from visually evoked fields) in the 2 task conditions, respectively, relative to the baseline trials (no targets). Figure 2, top row, presents the results of this analysis for the Target-Left condition. Panel *A*, illustrating the alpha topography for the first retention interval (one-target memory: delay 1), shows a clear decrease in alpha-band activity relative to baseline, strongest over the parietal areas in the right hemisphere.

What happens when the location of a second saccade target must be stored in memory? Panel *B*, showing alpha changes for the second memory period (2-target memory: delay 2), demonstrates a further but bilateral suppression of alpha relative to baseline over the posterior areas. Panel *C* then shows the effect of target load by plotting the difference in alpha power for the 2-target and the one-target load in the Target-Left condition (delay 2–delay 1). As this plot shows, alpha power decreases with increasing target load but almost equally in the posterior areas of both hemispheres.

Figure 2, middle row, shows the same analysis for the memory intervals in the Target-Right condition. Again, in this condition, alpha power decreases in the hemisphere contralateral to the remembered target location (panels *D* and *E*). The effects of target load, depicted in panel *F*, are consistent with the pattern in *C* showing that alpha power decreases with increasing memory demands. Although this effect can be seen in both hemispheres, the alpha decrease is most notable in the right (ipsilateral) hemisphere.

To determine the spatial selectivity of memory storage in more detail, we compared the alpha power for the Target-Left and Target-Right conditions. Thus, we subtracted the alpha activity for targets in the right visual field from the activity for targets in the left visual field. The results are depicted in Figure 2, bottom row, showing a clear contralateral suppression of alpha power for both the one-target memory interval (delay 1, panel G) and the 2-target memory period (delay 2, panel H). Blue regions indicate a stronger suppression for remembered target locations to the left than to the right of fixation, and vice versa for red regions. Note the hemispheric asymmetry in the pattern of alpha suppression. The suppression seems stronger and to cover a larger region in the left hemisphere than in the right. But clearly, alpha is suppressed in the hemisphere contralateral to the hemifield of stimulus presentation, most prominently over the sensors marked by the open circles. Consistent with these observations, a repeated-measures multivariate analysis of variance (MANOVA) over these sensors, with hemisphere (left/right) and target location (left/right hemifield) as factors, revealed a significant 2-way interaction for both the one-target memory period ($F_{1,7}$ = 11.7, P = 0.011) and the 2-target memory period ($F_{1,7}$ = 9.6, P = 0.018). Finally, Figure 2(I) demonstrates the interaction between the laterality effects and target load. As shown, the degree of laterality did virtually not depend on target load; if anything, it seems reduced during the 2-target memory period. Thus, in summary, 1) alpha is suppressed in the hemisphere contralateral to the hemifield of stimulus presentation and 2) alpha power decreased with the same amount in both hemispheres, when memory load is increased from one to two target locations.

Where in the brain can the oscillatory sources be identified that account for the contralateral suppression in the alpha band, as depicted in Figure 2? Spatial filtering based on the cross-spectral density matrix ("beamforming," see Methods) was used to estimate the sources in the brain that gave rise to the laterality effects in the alpha band, as observed on the scalp (Fig. 2G,H). Figure 3 provides an overview of these results based on standardized averaged group results, for the one-target memory (Fig. 3A) and the 2-targets memory period (Fig. 3B), showing only significant clusters of voxels based on a randomization analysis correcting for multiple comparisons (P < 0.05). Again, as in Figure 2(G,H), blue regions show a stronger suppression to leftward than rightward targets, whereas red regions represent the opposite. As shown, in both Figure 3(A,B), widespread contralateral alpha suppression can be observed in extrastriate brain regions. More precisely, significant contralateral suppression extended from close to the intraparietal and parietal–occipital sulcus into anterior-occipital cortex. It should also be noted that no such bilateral topographic regions were identified in frontal cortex, in this frequency range.

Thus far, the tuning and target load effects in the alpha band were observed as averaged effects during the retention periods. To determine the temporal evolution of the alpha activity, Figure 4 demonstrates the alpha topography at various time intervals of the Target-Left and Target-Right condition (2 upper rows), as well as the difference between them (bottom row). As shown, alpha modulations with respect to the baseline trials were absent just before and during the onset of the first stimulus (–0.2 to 0.2 s). Then, at the first 400 ms following the offset of the first stimulus, which characterizes the phasic response, there was a clear contralateral suppression in the alpha band at the posterior sensors, which was sustained at a slightly lower level throughout the first retention interval (0.6–2.0 s). Around the presentation of the second stimulus, alpha activity increased again but remained below baseline level. At the intervals of the second retention period, 2.4–2.8 s and 2.8–4.2 s, respectively, there were similar phasic and tonic responses. Finally, at the end of the trial, at the onset of the eye movements, alpha suppression vanished, as if alpha played no role in actually executing the response.

The effects described above were not restricted to the alpha band. Also the beta band (13–25 Hz) showed clear suppression effects, which became stronger after presentation of the second target, with a similar topography as the alpha band. This is shown in Figure 5, in the same format as in Figure 2. Compared with the alpha band, however, the degree of laterality was less robust. A repeated-measures MANOVA over the selected sensors (open circles), with hemisphere (left/right) and target location (left/right hemifield) as factors, revealed only a significant 2-way interaction for the one-target memory period ($F_{1,7}$ = 6.4, P = 0.039). Laterality of the activity during the 2-target memory period remained below statistical significance ($F_{1,7}$ = 4.0, P = 0.087).

Figure 6(A) (top panel) illustrates TFR of power difference between the Target-Left and Target-Right conditions for frequencies between 1 and 30 Hz, for the sensors marked in Figure 2. Data are presented in a pooled comparison across hemispheres computed as the power difference between contralateral and ipsilateral target conditions for each sensor, which was then averaged across all selected sensors and subjects. The bottom panel illustrates the statistically significant time–frequency clusters based on a cluster-randomization approach for multiple comparisons (P < 0.05, see Methods). The contralateral suppression effects are significant in the alpha and beta bands, as described above. In the beta band, the sustained, tonic component seems much weaker than the phasic component, suggesting that it may not be related to memory retention. Furthermore, with the frequency range 1–8 Hz there was a significant contralateral transient enhancement of activity in the theta range (at about 5 Hz) in response to each of the contralateral 2 cues (see dashed areas). This activity is most likely a contribution of a visually evoked field as it does not persist into the memory period.

Figure 6(B) shows the pattern of hemispheric laterality for the higher frequency bands (gamma band), in the same format as Figure 6(A). Enhancements can be discerned in response to both stimuli, with P < 0.1 for the first cue and P < 0.05 for the second cue but note that these enhancements are not retained into the memory periods. In fact, the first delay period does not show any significant power component within this frequency range. The second delay period, however, does demonstrate clear and significant (P < 0.05) lateralized activity, around 60–90 Hz, in a 1-s period prior to the initiation of the saccades.

To further examine this locus of activity, Figure 7(A) demonstrates the power modulations in the higher frequency band (gamma band) relative to baseline, for the same sensors showing contralateral alpha and beta suppression (see Fig. 7B). Data are plotted as an average across both hemispheres, that is, power differences (relative to baseline) were computed for contralateral and ipsilateral target conditions averaged across all selected sensors and subjects. The top and bottom panels show the power changes in response to targets presented in the contralateral and ipsilateral hemifield, respectively. Those power changes are expressed as z-scores relative to baseline trials.
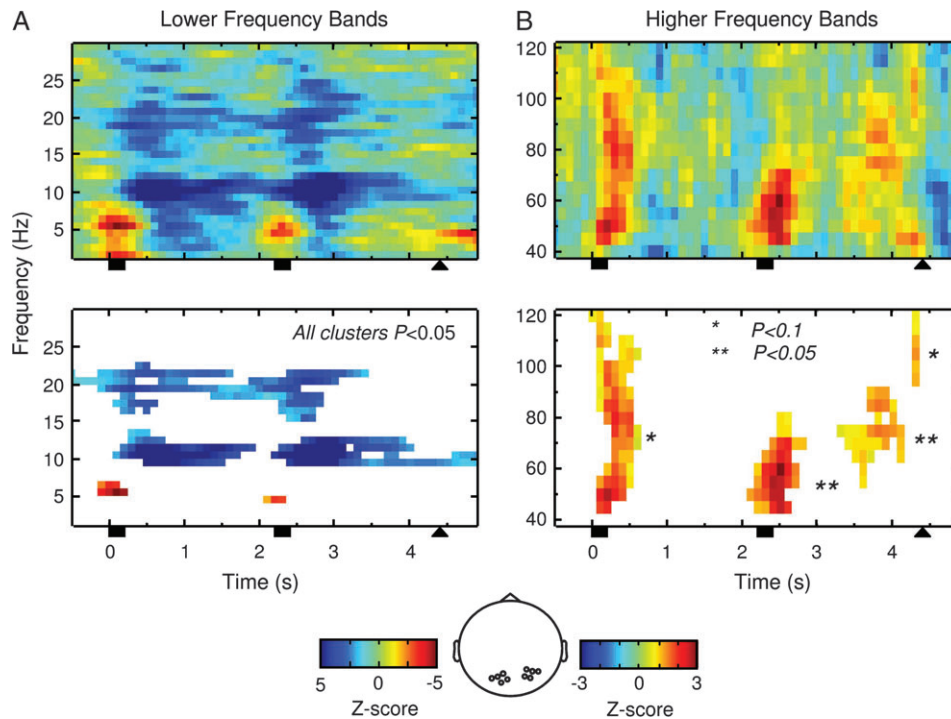
Figure 6. Spatial selectivity in lower and higher frequency bands in a pooled comparison across hemispheres. Time–frequency resolved power changes for the sensors marked in the bottom center panel. (*A*) Lower frequency bands. (*B*) Higher frequency bands. Top panels, complete TFR statistics; bottom panels, significance TFR regions (* clusters with $P < 0.1$, ** clusters with $P < 0.05$, cluster-randomization statistics). Squares: Time of the 2 cues. Triangle: Go cue for the saccades.

They demonstrate enhancements at about 40–60 Hz, prior to the presentation of the first stimulus. Those enhancements likely reflect the anticipation of a test trial as opposed to a baseline trial. Also, following the go cue for the saccades, a substantial gamma-band component can be noticed. More importantly, however, power in the gamma band was reduced relative to baseline during the first delay period, irrespective of whether a contralateral or an ispilateral target was kept in memory. During the second delay period, gamma power remained at a negative level when 2 ipsilateral targets were memorized but increased during the memory of 2 contralateral targets, most prominently in the frequency range 60–90 Hz and toward the end of the second delay period. As such, this would explain the findings of Figure 6(*B*): The gamma band shows a general desynchronization during the delay intervals, with less desynchronization for contralateral than ipsilateral targets during the second delay period. This observation is replotted in Figure 7(*C*), only for the second delay period and clusters that are significant at $P < 0.05$. It clearly shows that the gamma-band lateralization was not sustained during the entire duration of the period but arises at some point in time during the second delay period, perhaps when subjects start planning their saccades. In this respect, the contralateral gamma effects during the second delay period may reflect a neuronal correlate for preparatory set associated with saccade direction (Pesaran et al. 2002).

Discussion

We have investigated modulations of power in various frequency bands when subjects are processing and storing spatial information in a delayed double-step saccadic working memory task. To do so, we used a slightly modified version of the double-saccade experiment by Medendorp et al. (2006) performed in fMRI. Subjects were tested in a paradigm that employed 2-s delays between the occurrence of the first target, the second target, and the saccadic responses. In effect, this paradigm allowed us to dissociate the modulations in spectral power related to the first target (one-target memory load) and the first and second targets together (2-targets memory load). Our results showed a significant spatially selective suppression of power in the alpha and beta bands over posterior sensors during spatial working memory maintenance. This suppression was strongest over the hemisphere contralateral to the hemifield of the presented cue. We further found that oscillatory power in these bands decreased after presentation of the second cue but this memory effect itself did not exhibit any clear laterality. We localized the neural sources of these effects in parietal and occipital areas. Working memory maintenance of one target reduced also higher frequency (40–120 Hz) power over posterior sensors. However, in comparison with one-target memory, 2-target memory led to an increased gamma-band (60–90 Hz) power in the hemisphere contralateral to the targets, most notable shortly before the initiation of the saccades.

Let us now discuss the putative roles of the observed rhythms and their relation to previous interpretations. Recent studies, simultaneously recording electrophysiological and hemodynamic signals, have shown negative correlations between hemodynamic signals and spectral power in the alpha band (8–12 Hz) (Goldman et al. 2002; Laufs et al. 2003; Moosmann et al. 2003) but positive correlations in the gamma band (30–90 Hz) (Logothetis et al. 2001; Niessing et al. 2005). On this basis, our sources for lateralized alpha suppression in anterior-occipital and posterior parietal cortex are consistent with findings of recent fMRI studies that reported enhanced and directionally
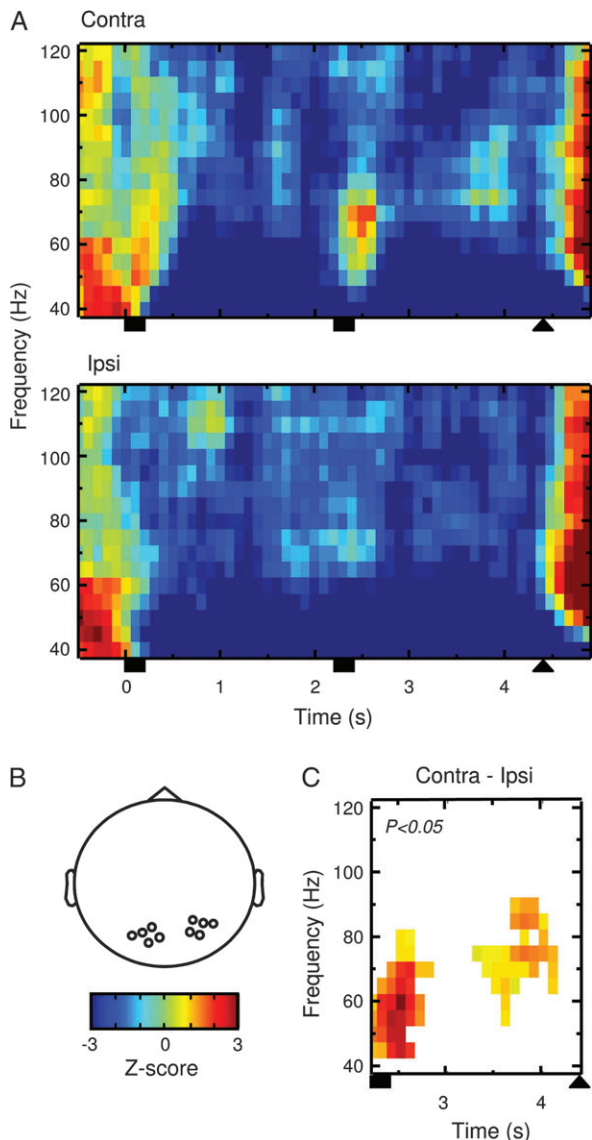
Figure 7. TFR of power in the higher frequency bands (40–120 Hz). (*A*) Gamma-band power relative to baseline. Data averaged across hemispheres for targets in the contralateral (top panel) and ipsilateral hemifield (bottom panel). (*B*) Sensors involved in the time–frequency analysis. (*C*) Gamma-band laterality at $P < 0.05$ during the second delay period, replotted from Figure 6(*B*). Squares: Time of the 2 cues. Triangle: Go cue for the saccades.

selective BOLD activation at virtually the same locations during the retention of a working memory for delayed saccades (Sereno et al. 2001; Medendorp et al. 2003, 2005; Koyama et al. 2004; Schluppeck et al. 2005). Also several studies using macaque monkeys have described areas at similar locations showing sustained activity during the memory period in delayed-saccade tasks, including extrastriate area V3A (Nakamura and Colby 2000) and posterior parietal area LIP (Barash et al. 1991; Colby et al. 1996; Mazzoni et al. 1996; Pesaran et al. 2002). The lateralized enhancement in gamma-band power during the second delay period compared with the first delay period also corroborates previous fMRI findings (Medendorp et al. 2006) showing directional-selective increases in BOLD activation in human posterior parietal cortex with memory load in a double-saccade task. Even the apparent gamma depression during the one-target

memory (Fig. 7) does not necessarily disagree with earlier findings but can be explained by the difference in spatial resolution between BOLD and MEG imaging, as we will further argue below. All together, our findings are well in accord with the notion that a decrease in alpha activity and increase in gamma-band activity reflect the engagement of a cortical region whose neural activity can also be measured as an increased BOLD signal or discharge rate in a spatial working memory task.

A reduction in alpha power is generally interpreted as a marker of activated brain regions (Singh et al. 2002). Areas not processing sensory information or motor output have been shown to retain increased power in the alpha band. Basically, our results showing clear suppression of alpha compared with its level obtained in the separate baseline trials are in support of this view. Our results also show that alpha is selectively suppressed in specific posterior regions, with more suppression in the hemisphere contralateral to the target. Again, this is compatible with the idea that activated brain regions are characterized by a reduction of alpha-band activity.

Our alpha findings confirm the results of Okada and Salenius (1998), who found a sustained suppression of alpha-band activity during a spatial working memory task, most prominently over posterior areas. Which role should be attributed to the sustained component? When subjects in the Okada and Salenius study passively viewed the stimuli, the sustained suppression was no longer present. This suggests that the tonic alpha decrease is involved in a function that transcends simple visual analysis. Worden et al. (2000) found this marker of neural processing to be directionally selective in a spatial attention task, with more alpha suppression over posterior cortex contralateral to the direction of attention (see also Sauseng et al. 2005; Kelly et al. 2006). Our findings add the notion that alpha power suppression is also lateralized during the coding of working memory for saccades. This is compatible with the idea that coding attention and planning saccades involve the same neural network (Posner et al. 1980; Rizzolatti et al. 1987; Findlay and Walker 1999).

Is the reduction in alpha a specific prerequisite for maintaining a working memory, or just a general mechanism operative to put particular brain areas into function? Working memory studies have revealed variable results as to the activity in the alpha band. Jensen et al. (2002) reported increases in alpha with memory load in a Sternberg task with letters. The same was found by Krause et al. (1996) in an auditory memory task. Also Klimesch et al. (1999) found alpha activity to be enhanced with working memory demands. By contrast, Gevins et al. (1997) reported decreased alpha in an *n*-back spatial working memory paradigm. Also the present study was performed in the spatial domain. The picture arising from these various results is that alpha is reduced when spatial functions are to be performed, whereas it is increased during nonspatial working memory tasks.

This basic result is incompatible with the notion of alpha activity as a general mechanism of working memory representations. In the same vein, it cannot be interpreted in support of the idling hypothesis (reviewed in Pfurtscheller et al. 1996). Rather, it argues in favor of a regulatory mechanism, put in place to allocate resources processing visuospatial information (Kelly et al. 2006; Thut et al. 2006). This puts forward a striking analogy with the classical idea that spatial and nonspatial functions are segregated in the brain, within a dorsal pathway and a ventral pathway, respectively (Ungerleider and Mishkin 1982). We propose that the alpha decrease during spatial working memory maintenance is due to an engagement of the dorsal stream.

Within this context, it can then be easily understood that the degree of alpha synchronization depends on the nature of the memory task. The increase in alpha power with working memory load during maintenance of letters or faces (Jensen et al. 2002) is due to an inhibition of the dorsal stream while the ventral stream is being engaged. More studies are required to test if this relationship holds up in general.

Interestingly, in the present study, we found that the degree of alpha lateralization did not further increase with target load, even though the alpha power was bilaterally reduced after presentation of the second target (Fig. 2). One possible reason for this effect is that the observed alpha laterality reflects anticipation of the second target (Worden et al. 2000). That is, after presentation of the first target, subjects anticipate the presentation of the second target which will be in the same hemifield. It could also mean that the laterality relates to the encoding of the first target, which is the goal for the first action, and remains this even after the second target has been presented. If so, this would suggest that the modulation in alpha power cannot be explained by visuospatial processing alone, but is also due to target selection for saccades. To distinguish between these and other possible explanations it would be useful to repeat the experiment with the second target presented at a location randomized across the 2 hemifields (Medendorp et al. 2006).

Virtually the same sensors showing alpha laterality also exhibited contralateral suppression effects of power in the beta-band (Fig. 5). This finding is consistent with numerous earlier studies reporting beta-band desynchronization in activated brain regions. Specifically, beta-band power over sensorimotor cortex of humans was found reduced during hand movements (Salmelin et al. 1995), beta-band activity in visual cortex was reduced during visual stimulation (Hoogenboom et al. 2006), and beta-band activity over typical language areas was reduced during language tasks (Ressel et al. 2006).

It has often been found that a desynchronization in the lower frequency bands (alpha, beta) goes hand-in-hand with synchronization in the higher frequency bands (gamma) (Munk et al. 1996; Fries et al. 2001; Schoffelen et al. 2005; Bauer et al. 2006; Hoogenboom et al. 2006). Moreover, several reports have suggested that oscillatory firing in the gamma band may be significant for active memory maintenance in delayed response tasks (Tallon-Baudry et al. 1998, 2001; Pesaran et al. 2002; Howard et al. 2003). For example, Tallon-Baudry et al. (1998) have reported clear enhancements of gamma-band activity in occipitotemporal and frontal regions during the delay in the memory condition of a delayed-matching-to-sample task with visual shapes. Pesaran et al. (2002) found that, during delays when monkeys are planning a saccade, there are broadband gamma oscillations (25–90 Hz) in the local field potentials (LFP) of posterior parietal area LIP. They found the LFP tuned to the direction of planned movements, changing its strength with behavioral state. Therefore, at first, one might be surprised by the predominant decrease of power in the gamma band during the memory periods in the present oculomotor paradigm (Fig. 7A). One possible explanation comes from recent evidence that local gamma enhancements are surrounded by more widespread gamma reductions (Lachaux et al. 2001; Shmuel et al. 2006). Studies using intracranial recordings typically do not see this effect, because they usually tailor stimulation to the recording site to obtain focal activation. Also BOLD-fMRI may attain high enough spatial resolution to not be contaminated by

these effects (Logothetis et al. 2001; Medendorp et al. 2006). However, MEG signals that average over a wider region of cortex might be dominated by the widespread gamma reduction in the surround such that the net effect at the MEG sensor is a gamma power reduction. This notion is fully compatible with our finding that contralateral gamma-band power did increase during the second delay period as compared with the first (see Figs 6B and 7C). The available evidence suggests that gamma-band synchronization in the absence of appropriate stimuli or tasks is weak. It is thus reasonable to assume that the gamma desynchronization (surrounding a focal synchronization) essentially abolishes any (nonspurious) gamma-band synchronization in the surround. As a consequence, the resulting level of minimal gamma-band synchronization would not be further reduced even if more focal activations would be added, as, for example, in our case by adding the second target. This model can explain the observations in the gamma-band: The first target induces one focus of enhanced gamma synchronization surrounded by widespread gamma desynchronization with the net effect at the MEG sensor of reduced gamma power. The second target adds a second focus of enhanced gamma synchronization, while the surround is already completely desynchronized and does not desynchronize further. The net effect at the MEG sensor is an increase in gamma power relative to the first target. It remains important to emphasize that the increased activity did not occur over the total duration of the second delay period, but only arose shortly before the initiation of the saccades. In a strict interpretation, the laterality effects that are observed during the second delay period do not so much reflect a target load effect but perhaps more so a motor planning effect, which would be consistent with the findings by Pesaran et al. (2002) for monkey parietal cortex.

In summary, the present study has provided evidence that changes in synchronized oscillatory neural activity are tuned to specific regions of space and modulated by target load during memory periods in an oculomotor task. Future research is required to determine more precisely how neural signals are processed in regions that are involved in storing and transforming spatial information into motor action.

Notes

Address correspondence to W. P. Medendorp, PhD, Nijmegen Institute for Cognition and Information, Radboud University Nijmegen, PO Box 9104, NL-6500 HE Nijmegen, The Netherlands. Email: p.medendorp@nici.ru.nl.

References

Andersen RA, Buneo CA. 2002. Intentional maps in posterior parietal cortex. Annu Rev Neurosci. 25:189–220.

Barash S, Bracewell RM, Fogassi L, Gnadt JW, Andersen RA. 1991. Saccade-related activity in the lateral intraparietal area. II. Spatial properties. J Neurophysiol. 66:1109–1124.

Bauer M, Oostenveld R, Peeters M, Fries P. 2006. Tactile spatial attention enhances gamma-band activity in somatosensory cortex and reduces low-frequency activity in parieto-occipital areas. J Neurosci. 26:490–501.

Ben Hamed S, Duhamel JR, Bremmer F, Graf W. 2001. Representation of the visual field in the lateral intraparietal area of macaque monkeys: a quantitative receptive field analysis. Exp Brain Res. 140:127-144.

Blatt GJ, Andersen RA, Stoner GR. 1990. Visual receptive field organization and cortico-cortical connections of the lateral intraparietal area (area LIP) in the macaque. J Comp Neurol. 299:421-445.

Colby CL, Duhamel JR, Goldberg ME. 1996. Visual, presaccadic, and cognitive activation of single neurons in monkey lateral intraparietal area. J Neurophysiol. 76:2841-2852.

Efron B, Tibshirani R. 1991. Statistical data analysis in the computer age. Science. 253:390-395.

Engel AK, Fries P, Singer W. 2001. Dynamic predictions: oscillations and synchrony in top-down processing. Nat Rev Neurosci. 2:704-716.

Findlay JM, Walker R. 1999. A model of saccade generation based on parallel processing and competitive inhibition. Behav Brain Sci. 22:661-674.

Fries P, Reynolds JH, Rorie AE, Desimone R. 2001. Modulation of oscillatory neuronal synchronization by selective visual attention. Science. 291:1560-1563.

Gevins A, Smith ME, McEvoy L, Yu D. 1997. High-resolution EEG mapping of cortical activation related to working memory: effects of task difficulty, type of processing, and practice. Cereb Cortex. 7:374-385.

Goldman RI, Stern JM, Engel J Jr, Cohen MS. 2002. Simultaneous EEG and fMRI of the alpha rhythm. Neuroreport. 13:2487-2492.

Gross J, Kujala J, Hämäläinen M, Timmermann L, Schnitzler A, Salmelin R. 2001. Dynamic imaging of coherent sources: studying neural interactions in the human brain. Proc Natl Acad Sci USA. 98:694-699.

Hamalainen M, Hari R, Ilmoniemi R, Knuutila J, Lounasmaa O. 1993. Magnetoencephalography—theory, instrumentation, and applications to noninvasive studies of the working human brain. Rev Mod Phys. 65:1-93.

Hari R, Salmelin R. 1997. Human cortical oscillations: a neuromagnetic view through the skull. Trends Neurosci. 20:44-49.

Hoogenboom N, Schoffelen JM, Oostenveld R, Parkes LM, Fries P. 2006. Localizing human visual gamma-band activity in frequency, time and space. Neuroimage. 29:764-773.

Howard MW, Rizzuto DS, Caplan JB, Madsen JR, Lisman J, Aschenbrenner-Scheibe R, Schulze-Bonhage A, Kahana MJ. 2003. Gamma oscillations correlate with working memory load in humans. Cereb Cortex. 13:1369-1374.

Huang M, Mosher JC. 1997. A novel head model for the MEG forward problem: BEM accuracy with only spherical model complexity. Neuroimage. 5:441.

Jensen O, Gelfand J, Kounios J, Lisman JE. 2002. Oscillations in the alpha band (9-12 Hz) increase with memory load during retention in a short-term memory task. Cereb Cortex. 12:877-882.

Kaiser J, Ripper B, Birbaumer N, Lutzenberger W. 2003. Dynamics of gamma-band activity in human magnetoencephalogram during auditory pattern working memory. Neuroimage. 20:816-827.

Kelly SP, Lalor EC, Reilly RB, Foxe JJ. 2006. Increases in alpha oscillatory power reflect an active retinotopic mechanism for distracter suppression during sustained visuo-spatial attention. J Neurophysiol. 95:3844-3851.

Klimesch W. 1999. EEG alpha and theta oscillations reflect cognitive and memory performance: a review and analysis. Brain Res Brain Res Rev. 29:169-195.

Klimesch W, Doppelmayr M, Schwaiger J, Auinger P, Winkler T. 1999. 'Paradoxical' alpha synchronization in a memory task. Brain Res Cogn Brain Res. 7:493-501.

Koyama M, Hasegawa I, Osada T, Adachi Y, Nakahara K, Miyashita Y. 2004. Functional magnetic resonance imaging of macaque monkeys performing visually guided saccade tasks: comparison of cortical eye fields with humans. Neuron. 41:795-807.

Krause CM, Lang AH, Laine M, Kuusisto M, Porn B. 1996. Event-related EEG desynchronization and synchronization during an auditory memory task. Electroencephalogr Clin Neurophysiol. 98:319-326.

Lachaux JP, George N, Tallon-Baudry C, Martinerie J, Hugueville L, Minotti L, Kahane P, Renault B. 2005. The many faces of the gamma band response to complex visual stimuli. Neuroimage. 25:491-501.

Laufs H, Kleinschmidt A, Beyerle A, Eger E, Salek-Haddadi A, Preibisch C, Krakow K. 2003. EEG-correlated fMRI of human alpha activity. Neuroimage. 19:1463-1476.

Lee H, Simpson GV, Logothetis NK, Rainer G. 2005. Phase locking of single neuron activity to theta oscillations during working memory in monkey extrastriate visual cortex. Neuron. 45:147-156.

Logothetis NK, Pauls J, Augath M, Trinath T, Oeltermann A. 2001. Neurophysiological investigation of the basis of the fMRI signal. Nature. 412:150-157.

Lutzenberger W, Ripper B, Busse L, Birbaumer N, Kaiser J. 2002. Dynamics of gamma-band activity during an audiospatial working memory task in humans. J Neurosci. 22:5630-5638.

Mazzoni P, Bracewell RM, Barash S, Andersen RA. 1996. Motor intention activity in the macaque's lateral intraparietal area. I. Dissociation of motor plan from sensory memory. J Neurophysiol. 76:1439-1456.

Medendorp WP, Goltz HC, Vilis T. 2005. Remapping the remembered target location for anti-saccades in human posterior parietal cortex. J Neurophysiol. 94:734-740.

Medendorp WP, Goltz HC, Vilis T. 2006. Directional selectivity of BOLD activity in human posterior parietal cortex for memory-guided double-step saccades. J Neurophysiol. 95:1645-1655.

Medendorp WP, Goltz HC, Vilis T, Crawford JD. 2003. Gaze-centered updating of visual space in human parietal cortex. J Neurosci. 23: 6209-6214.

Mitra PP, Pesaran B. 1999. Analysis of dynamic brain imaging data. Biophys J. 76:691-708.

Moosmann M, Ritter P, Krastel I, Brink A, Thees S, Blankenburg F, Taskin B, Obrig H, Villringer A. 2003. Correlates of alpha rhythm in functional magnetic resonance imaging and near infrared spectroscopy. Neuroimage. 20:145-158.

Munk MH, Roelfsema PR, Konig P, Engel AK, Singer W. 1996. Role of reticular activation in the modulation of intracortical synchronization. Science. 272:271-274.

Nakamura K, Colby CL. 2000. Visual, saccade-related, and cognitive activation of single neurons in monkey extrastriate area V3A. J Neurophysiol. 84:677-692.

Nichols TE, Holmes AP. 2002. Nonparametric permutation tests for functional neuroimaging: a primer with examples. Hum Brain Mapp. 15:1-25.

Niessing J, Ebisch B, Schmidt KE, Niessing M, Singer W, Galuske RA. 2005. Hemodynamic signals correlate tightly with synchronized gamma oscillations. Science. 309:948-951.

Okada YC, Salenius S. 1998. Roles of attention, memory, and motor preparation in modulating human brain activity in a spatial working memory task. Cereb Cortex. 8:80-96.

Osipova D, Takashima A, Oostenveld R, Fernandez G, Maris E, Jensen O. 2006. Theta and gamma oscillations predict encoding and retrieval of declarative memory. J Neurosci. 26:7523-31.

Pesaran B, Pezaris JS, Sahani M, Mitra PP, Andersen RA. 2002. Temporal structure in neuronal activity during working memory in macaque parietal cortex. Nat. Neurosci. 5:805-811.

Pfurtscheller G, Stancak A, Neuper C. 1996. Event-related synchronization (ERS) in the alpha band{an electrophysiological correlate of cortical idling: a review. Int J Psychophysiol. 24:39-46.

Pierrot-Deseilligny C, Milea D, Muri RM. 2004. Eye movement control by the cerebral cortex. Curr Opin Neurol. 17:17-25.

Platt ML, Glimcher PW. 1998. Response fields of intraparietal neurons quantified with multiple saccadic targets. Exp Brain Res. 121:65-75.

Posner MI, Snyder CR, Davidson BJ. 1980. Attention and the detection of signals. J Exp Psychol. 109:160-174.

Ressel V, Wilke M, Lidzba K, Preissl H, Krageloh-Mann I, Lutzenberger W. 2006. Language lateralization in magnetoencephalography: two tasks to investigate hemispheric dominance. Neuroreport. 17: 1209-1213.

Rizzolatti G, Riggio L, Dascola I, Umiltá C. 1987. Reorienting attention across the horizontal and vertical meridians: evidence in favor of a premotor theory of attention. Neuropsychologia. 25:31-40.

Salmelin R, Hámáaláinen M, Kajola M, Hari R. 1995. Functional segregation of movement-related rhythmic activity in the human brain. Neuroimage. 2:237-243.

Sauseng P, Klimesch W, Stadler W, Schabus M, Doppelmayr M, Hanslmayr S, Gruber WR, Birbaumer N. 2005. A shift of visual spatial attention is selectively associated with human EEG alpha activity. Eur J Neurosci. 22:2917-2926.

Scherberger H, Jarvis MR, Andersen RA. 2005. Cortical local field potential encodes movement intentions in the posterior parietal cortex. Neuron. 46:347–354.

Schluppeck D, Glimcher P, Heeger DJ. 2005. Topographic organization for delayed saccades in human posterior parietal cortex. J Neurophysiol. 94:1372–1384.

Schoffelen JM, Oostenveld R, Fries P. 2005. Neuronal coherence as a mechanism of effective corticospinal interaction. Science. 308:111–113.

Sereno MI, Pitzalis S, Martinez A. 2001. Mapping of contralateral space in retinotopic coordinates by a parietal cortical area in humans. Science. 294:1350–1354.

Shmuel A, Augath M, Oeltermann A, Logothetis NK. 2006. Negative functional MRI response correlates with decreases in neuronal activity in monkey visual area V1. Nat Neurosci. 9:569–577.

Singh KD, Barnes GR, Hillebrand A, Forde EM, Williams AL. 2002. Task-related changes in cortical synchronization are spatially coincident with the hemodynamic response. Neuroimage. 16:103–114.

Tallon-Baudry C, Bertrand O, Delpuech C, Pernier J. 1996. Stimulus specificity of phase-locked and non-phase-locked 40 Hz visual responses in human. J Neurosci. 16:4240–4249.

Tallon-Baudry C, Bertrand O, Fischer C. 2001. Oscillatory synchrony between human extrastriate areas during visual short-term memory maintenance. J Neurosci. 21:RC177.

Tallon-Baudry C, Bertrand O, Peronnet F, Pernier J. 1998. Induced gamma-band activity during the delay of a visual short-term memory task in humans. J Neurosci. 18:4244–4254.

Thut G, Nietzel A, Brandt SA, Pascual-Leone A. 2006. {alpha}-Band electroencephalographic activity over occipital cortex indexes visuospatial attention bias and predicts visual target detection. J Neurosci. 26:9494–9502.

Ungerleider LG, Mishkin M. 1982. Two cortical visual systems. In: Ingle DJ, Goodale MA, Mansfield RJW, editors. Analysis of visual behavior. MIT Press, Cambridge, MA. p. 549–586.

Van Veen BD, van Drongelen W, Yuchtman M, Suzuki A. 1997. Localization of brain electrical activity via linearly constrained minimum variance spatial filtering. IEEE Trans Biomed Eng. 44:867–880.

Worden MS, Foxe JJ, Wang N, Simpson GV. 2000. Anticipatory biasing of visuospatial attention indexed by retinotopically specific alpha-band electroencephalography increases over occipital cortex. J Neurosci. 20:RC63.